



ELSEVIER



Long-term studies on the integration of acellular porcine dermis as an implant shell and the effect on capsular fibrosis around silicone implants in a rat model

I. Ludolph^{a,*}, J.S. Gruener^a, A. Kengelbach-Weigand^a,
C. Fiessler^b, R.E. Horch^a, M. Schmitz^a

^aDepartment of Plastic and Hand Surgery and Laboratory for Tissue Engineering and Regenerative Medicine, University Hospital of Erlangen, Friedrich-Alexander-University of Erlangen-Nürnberg (FAU), Krankenhausstraße 12, 91054 Erlangen, Germany

^bInstitute for Medical Informatics, Biometry, and Epidemiology, Friedrich-Alexander-University of Erlangen-Nürnberg (FAU), Wetterkreuz 13, 91058 Erlangen, Germany

Received 10 August 2018; accepted 23 April 2019

KEYWORDS

Capsular fibrosis;
Capsular contracture;
Acellular porcine;
Dermal matrix;
Breast reconstruction

Summary Acellular dermal matrices have recently increasingly been used in alloplastic breast reconstruction with silicone breast implants. Among these matrices, acellular porcine dermis (APD) is frequently applied, but long-term data on tissue integration and capsular fibrosis formation are still missing.

Silicone prostheses with (group A) and without (group B) APD as an implant-covering shell were implanted in male Lewis rats. At 3, 12, and 52 weeks after implantation, the constructs were explanted. Molecular biological and immunohistochemical analyses were performed afterwards.

On comparing the collagenous layer and the newly formed myofibroblast-rich layer around the implants of both groups, it became apparent that in group A, these layers were thinner, followed by a lower expression of TGF β 1 after 12 and 52 weeks. Further, in this group, at the endpoint of 52 weeks, a lower amount of CD68-positive cells in the collagenous and myofibroblast-rich layers were observed and the expression of TNF α was reduced, while the number of Ki67-positive cells was significantly higher with time. Furthermore, MMP1 expression

Parts of this article have been presented at the following meetings/conferences: 1. 47th Congress of the German Society of Plastic, Reconstructive and Aesthetic Surgeons 8 September–10 September 2016, Kassel, Germany. 2. The 36th Congress of the German Society of Senology, 26 May–28 May 2016, Dresden, Germany.

*Corresponding author.

E-mail address: ingo.ludolph@uk-erlangen.de (I. Ludolph).

<https://doi.org/10.1016/j.bjps.2019.04.015>

1748-6815/© 2019 British Association of Plastic, Reconstructive and Aesthetic Surgeons. Published by Elsevier Ltd. All rights reserved.

in group A was lower than that in group B, and the calculated ratio of MMP1:TIMP1 expression was higher.

The long-term results clearly show a reduction in inflammatory and fibrotic tissue reaction when APD is used to cover silicone prostheses. These experimental data will be of considerable importance for implant-based breast surgery, as they indicate a potential benefit in the reduction of capsular fibrosis formation of an interposition of APD between the recipient and the silicone implant.

© 2019 British Association of Plastic, Reconstructive and Aesthetic Surgeons. Published by Elsevier Ltd. All rights reserved.

Introduction

Silicone breast implants are frequently used for both esthetic and reconstructive reasons. However, one of the major lasting problems in using silicone implants is the development of capsular contracture, which causes implant deformities and breast pain in advanced stages.^{1,2}

Biological implants such as allogenic, porcine, or bovine acellular dermal matrices are commonly used to create a biological interface between the implant and the host tissue with the aim of reducing capsular contracture and to provide additional cover between the implant and the skin envelope.³⁻⁵ Particularly, in alloplastic breast reconstruction after mastectomy, they are also applied to reconstruct an undefined inframammary fold.

Different hypotheses exist concerning the pathomechanism of capsular contracture, yet none of them has been clearly verified to date.^{6,7} In experimental studies on human capsule explants, as well as in animal models, certain tissue reactions in the capsular tissue were described at both a molecular biological and an immunohistochemical level, whereas questions of microorganism-induced chronic inflammation in a biofilm have not yet been definitely answered for clinical daily routine. Therefore, to date, no true causal therapy or prophylaxis exists.⁸⁻¹¹ Use of acellular porcine dermis (APD) to overcome such problems has been investigated in a considerable number of clinical trials, case reports, and case series.¹²⁻¹⁵ However, the number of experimental studies to clarify the influence of APD in preventing capsular contracture is still limited. In particular, no experimental longitudinal analysis exceeding a time span of more than 12 weeks has been published thus far.

The aim of this study was, therefore, to analyze molecular biological and cellular mechanisms concerning the development of capsular contracture in a rat model, using an APD as a full cover of silicone implants, and to evaluate the long-term results over a period of one year after implantation.

Materials and methods

To create an authentic model, slightly textured silicone testicular implants for pets with a length of 0.63 inches (Neuticles® UltraPLUS® XXSmall, Neuticles® CTI Corporation, Oak Grove, MO, USA) were implanted in young male Lewis rats (Charles River Laboratories, Sulzfeld, Germany).

Animal experiments were approved by the Institutional Animal Care and Use Committee of the Regierungspräsidium von Mittelfranken, Germany (no. 54-2532.1-50/13).

Two experimental groups were defined. In group A, implants were completely covered by a non-cross-linked APD matrix (Fortiva®, Tutogen Medical, Neunkirchen am Brand, Germany) (Figure 1). The scaffolds were sterilized by low-dose gamma irradiation. In group B, as the control, uncovered prostheses were implanted. Two prostheses from the same group were implanted in separate implant pockets under the muscle layer on the backs of the rats, the so-called panniculus carnosus. The explantation time points were set at 3, 12, and 52 weeks. At these points, 8 samples of each group (A and B) were assured.

All operations were performed under aseptic conditions. After initiating anesthesia with isoflurane inhalation (Forene 100%, Völtar GmbH, Hamburg, Germany), the rat was placed in the prone position and the back was shaved. Skin disinfection was performed with Cutasept F (Bode Chemie GmbH, Hamburg, Germany). For analgesia, 200 µl Rimadyl® Carprofen (Pfizer GmbH, Berlin, Germany) was injected subcutaneously, as well as 0.2 ml Veracin® (dihydrostreptomycin sulfate, procaine benzylpenicillin, and benzathine benzylpenicillin, Albrecht GmbH, Aulendorf, Germany) intramuscularly as antibiotic prophylaxis. Before implantation, the APD was wrapped around the prostheses, covering the complete silicone surface, and closed by a continuous suture with 4/0 polypropylene. A pocket was prepared under the panniculus carnosus by blunt dissection, and the prostheses with or without APD as an envelope were implanted. Skin closure was done with a 4/0 polyglactin suture (Vicryl® 4/0, Johnson & Johnson Medical GmbH, Ethicon Surgical Care, Norderstedt, Germany). Aluminum spray (Alu-Spray "trocken," Pharma-Partner Vertriebs-GmbH, Hamburg, Germany) was used as a wound dressing.

In the postoperative course, analgesia was administered through drinking water with tramadol hydrochloride (Tramal® Tropfen, Grünenthal, Aachen, Germany).

Explantation

The prostheses including the surrounding tissue (skin, subcutaneous tissue, and panniculus carnosus) were explanted after 3, 12, and 52 weeks and the animals sacrificed by administering an intracardiac injection of 0.5 ml T61® (Intervet Deutschland GmbH, Unterschleißheim, Germany) in deep anesthesia.



Figure 1 Left: slightly textured silicone testicular implants (0.63 in.). Middle: acellular porcine dermal matrix. Right: testicular implant totally wrapped by APD.

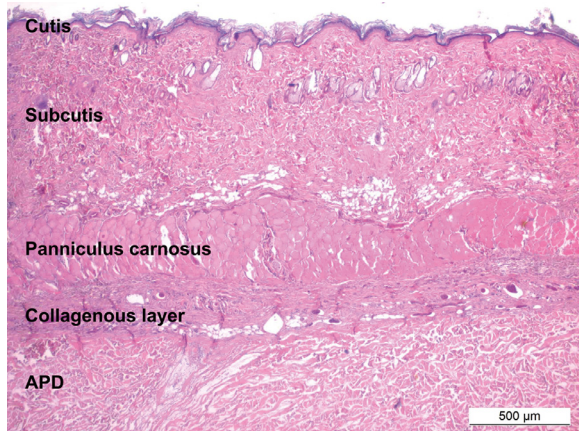


Figure 2 Histological overview in HE. From top to bottom: cutis, subcutis, panniculus carnosus, collagenous layer, and APD.

Tissue processing and histological and immunohistochemical staining

After extracting the prostheses, all samples were fixed in 4% formaldehyde (Roti-Histofix 4%, Carl Roth GmbH, Karlsruhe, Germany). Each sample was embedded in paraffin blocks after cutting into similar pieces. Using a rotary microtome (Thermo Fisher Scientific HM 355 S Automatic Microtome, Waltham, MA, USA), sections were made with a 2.5 μm layer thickness and attached to glass slides.

Histological staining with hematoxylin and eosin (HE) provided an overview for tissue/layer analysis (Figure 2). Immunohistochemical staining for cell proliferation was performed with Ki67 (Rabbit monoclonal-Anti-Ki67, Zytomed Systems GmbH, Berlin, Germany) and CD68 to visualize monocytes and macrophages as a marker of inflammation (Mouse antirat CD68, MCA341R, AbD Serotec, Raleigh, NC, USA). In addition, double staining of alpha smooth muscle actin (alpha-SMA, Mouse anti-Actin clone 1A4, smooth muscle, Zytomed Systems GmbH, Berlin, Germany) was performed and von Willebrand factor (vWF, Factor VIII, Biocare Medical Inc., Concord, CA, USA) was used for visualization of myofibroblasts and smooth muscle cells in vessel walls.

Morphometry

The results of the aforementioned staining were evaluated with a microscope system (Leica Leitz DM RBE and Leica DFC420, Leica Microsystems GmbH, Wetzlar, Germany). Furthermore, photographs were taken in 5 regions of interest using increased magnifications (Figure 3). For the histological overview and the collagenous layer in the HE staining, as well as for the vessels in the APD in the alpha-SMA and vWF staining, 100-fold magnification was used. Quantification analysis of the myofibroblast layer and CD68- and Ki67-positive cells was performed in 400-fold magnification (Figure 4). The thickness of the APD was measured in 25-fold magnification. CD68- and Ki67-positive cells were counted in each of the 5 regions of interest, and arithmetic mean was calculated for each sample followed by calculation of

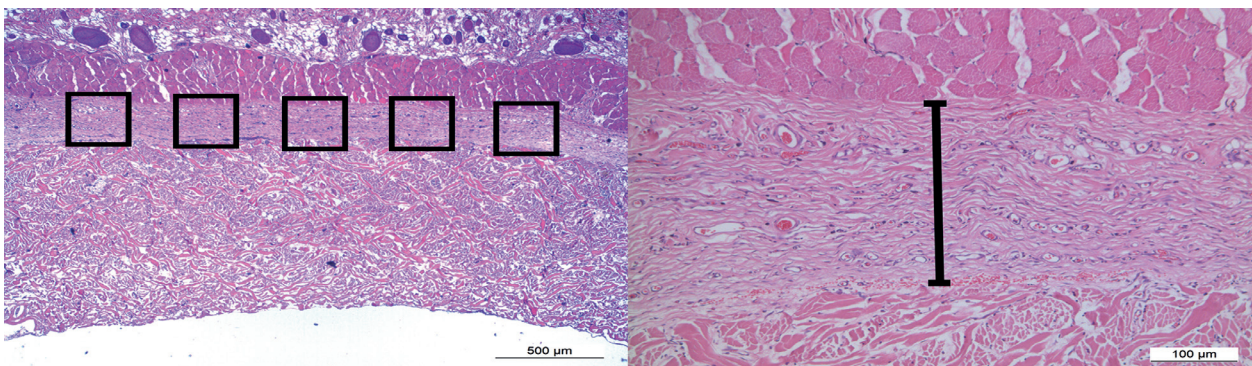


Figure 3 Left: HE staining with assessed regions of interest. Right: thickness of collagenous layer marked (HE staining).

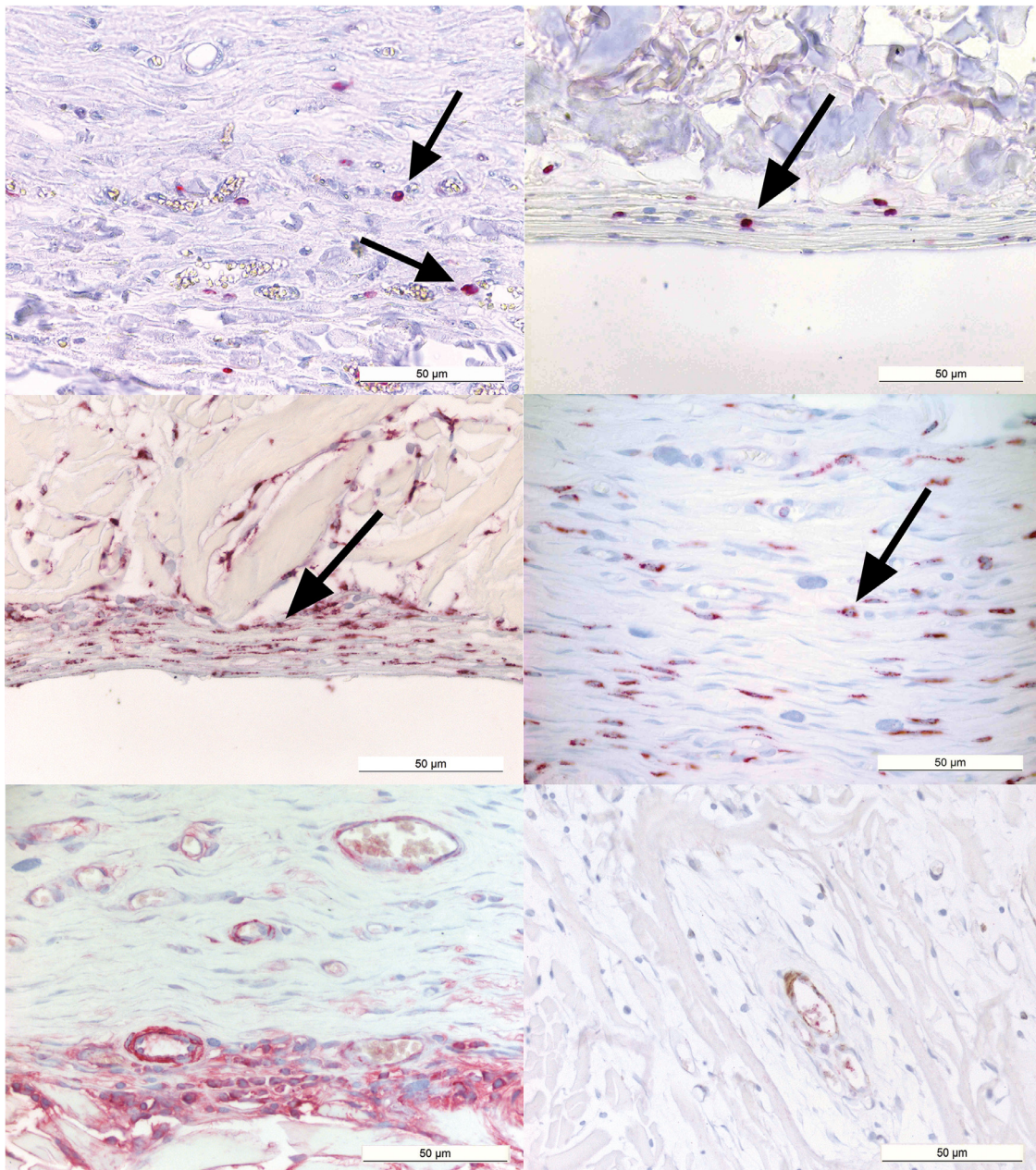


Figure 4 Top: Ki67-positive cells in the collagenous layer (left) and in the myofibroblast-rich layer (right) (arrows). Middle: CD68-positive cells in the collagenous layer (right) and in the myofibroblast-rich layer (left) (arrows). Bottom: myofibroblast-rich layer between collagenous layer (top) and APD (bottom) (left). Vessels in the APD (central) (right).

the arithmetic mean for all samples of the different study groups at the single explantation time points.

Real-time quantitative polymerase chain reaction (qPCR)

Quantification of the mRNA expression of $TGF\beta 1$, $TNF\alpha$, matrix metalloproteinase 1 (MMP1), and tissue inhibitor of MMP1 was performed by qPCR. After 3, 12, and 52 weeks, total RNA was extracted from both the experimental group and the control group. For this, a deparaffinization kit (QIAGEN GmbH, Hilden, Germany) was used for

the formalin-fixed paraffin-embedded blocks. The mRNA was isolated with RNeasy[®] FFPE Kit (QIAGEN GmbH, Hilden, Germany). Total mRNA was reverse transcribed into cDNA using the Sensiscript[®] Reverse Transcription Kit (QIAGEN GmbH, Hilden, Germany). All primer sequences are listed in Table 1. Real-time quantitative PCR was carried out using the SsoAdvanced[™] Universal SYBR[®] Green Supermix (Bio-Rad Laboratories Inc., Hercules, CA, USA) and a thermocycler (CFX96 Real-Time System C1000 Touch[™] Thermal Cycler, Bio-Rad Laboratories Inc., Hercules, CA, USA). All kits were used according to the manufacturers' protocols. Samples were tested as triplicates. The expression of each gene was normalized to that of the housekeeping gene

Table 1 Primer sequences for qPCR.

Gene	Forward primer (5'–3')	Reverse primer (5'–3')
GAPDH	CAACGACCCCTTCATTGACC	TTCTCAGCCTTGACTGTGCC
TGF β 1	TGGAGCCTGGACACACAGTA	TGTTGGTTGTAGAGGGCAAGG
TNF α	TCAGCCTCTTCTCATTCCCG	ACAGAAGAGCGTGGTGCC
MMP1	GGAAGGTGATATTGTGTTCCGCC	CTATGGTCTCTCTGTAGAAGGC
TIMP1	ACGCTAGAGCAGATACCACG	AGAGGCCAGAGATGCAAAGG

glyceraldehyde-3-phosphate dehydrogenase (GAPDH), and the evaluation was made by the 2-deltadeltaCt method.

Statistical analysis

Mean values of collagenous and myofibroblast-rich layer thickness and cell counts of CD68- and Ki67-positive cells were compared, descriptively stratified by group and explantation time points. Multivariable analysis was performed by computing generalized linear mixed models with random effects accounting for multiple measurements on the same implant. Thickness of the collagenous and the myofibroblast-rich layer was assumed to follow a log-normal distribution, whereas cell counts of CD68- and Ki67-positive cells were modeled with a negative binomial regression model due to overdispersion. Group and explantation time points, as well as an interaction time period to model time-dependent effects, were included in the regression analysis as predictor variables. Differences between the numbers of blood vessels in the APD at different explantation time points were evaluated by the Mann-Whitney test. Owing to multiple hypotheses analyzed in this study, *p* values should be considered as exploratory. All statistical analyses were conducted using the statistical software package R Version 3.2.2 (The R Foundation for Statistical Computing, Vienna, Austria).

Results

In all rats, operative and postoperative phases were uneventful. In the hematoxylin-eosin stained overview, the collagenous layer, which occurred in all samples in both groups, increased until the 12-week time point. After 52 weeks, this layer became thinner than that after the 3-week time point in the experimental group (A), whereas it remained almost at the same level in the control group (B). At every time point, the collagenous layer was shown to be significantly thinner in group A than in group B ($p < 0.05$) (Figure 5). Based on the alpha-SMA staining, a periprosthetic myofibroblast-rich layer was detected at the interface between the silicone implant and the APD (group A) and the collagenous layer (group B), respectively. After 12 weeks, the thickness increased in both groups but presented as 37% thicker in group B. In the long-term period, the thickness of the myofibroblast-rich layer decreased in group A almost to the initial level at 3 weeks. By contrast, this layer became consistently thicker in group B, showing a statistically significant difference ($p < 0.05$) (Figure 6). The cells showed a markedly homogeneous distribution within the single my-

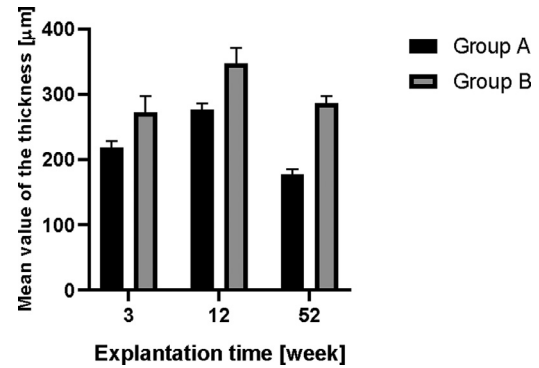


Figure 5 Results of the comparison of thickness of the collagenous layer in both groups and at 3 explantation time points from a descriptive analysis.

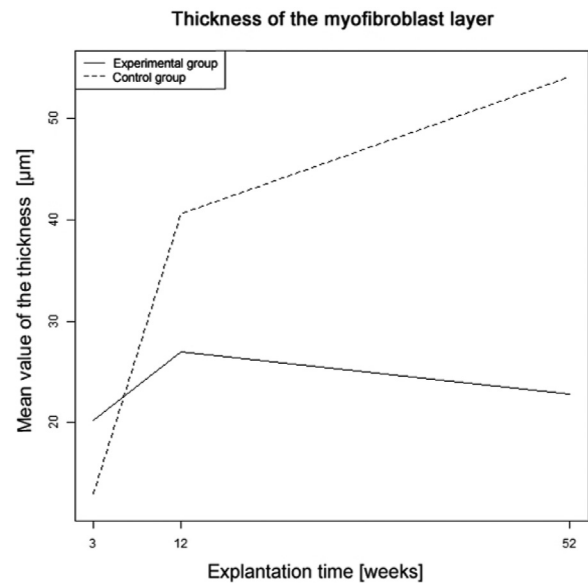


Figure 6 Results of the comparison of thickness of the myofibroblast-rich layer in both groups and at 3 explantation time points from a descriptive analysis.

ofibroblast layer and a consistent morphology. Furthermore, the relation of cells and extracellular matrix (ECM) was balanced. In addition, the same layer of myofibroblasts was seen between the APD matrix and the collagenous layer in group A at 3 and 12 weeks after implantation (peri-ADM layer). However, this peri-ADM layer was not present in all samples, and after 52 weeks, it was completely degraded.

The grade of proliferation shown by detection of Ki67-positive cells revealed an evident decrease in proliferating

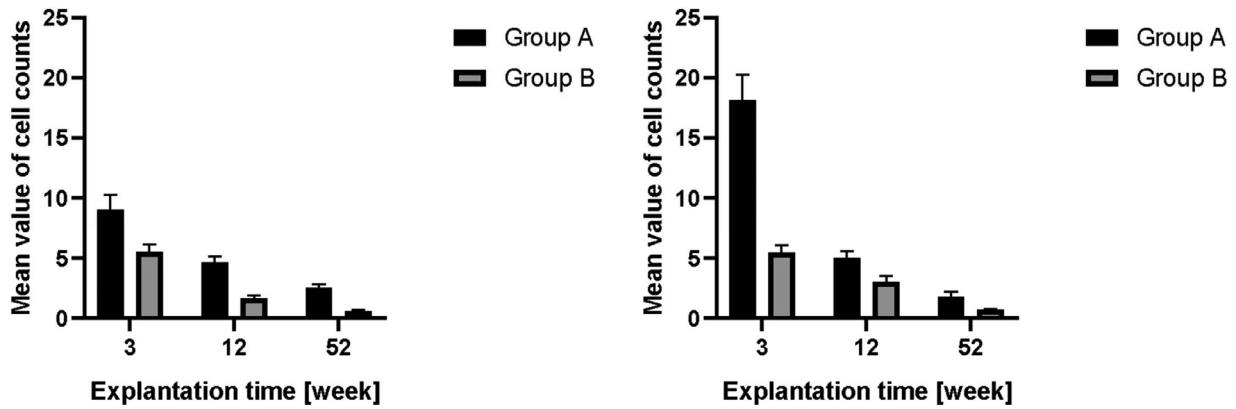


Figure 7 Results of the comparison of Ki67-positive cells in the collagenous layer (left) and in the myofibroblast-rich layer (right) in both groups and at 3 explantation time points from a descriptive analysis.

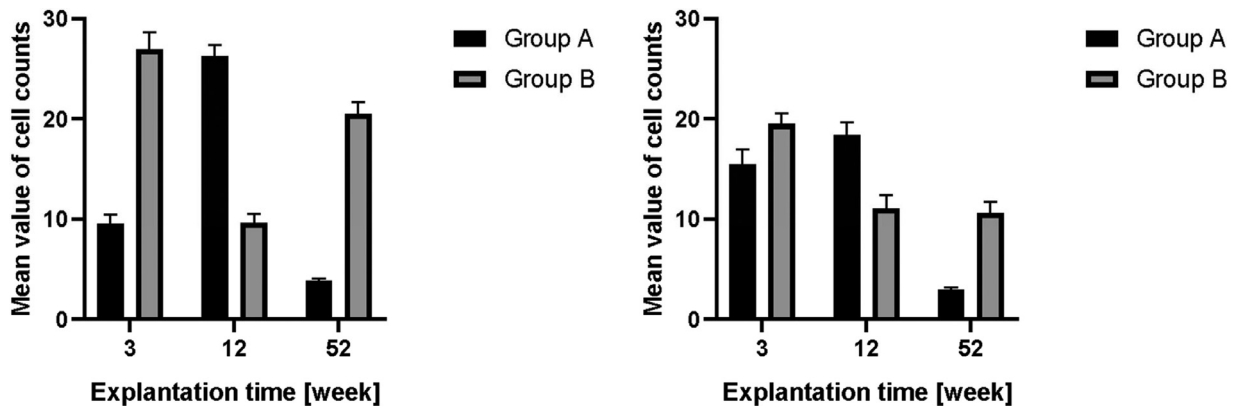


Figure 8 Results of the comparison of CD68-positive cells in the collagenous layer (left) and in the myofibroblast-rich layer (right) in both groups and at 3 explantation time points from a descriptive analysis.

cells with time, both in the collagenous and in the periprosthetic myofibroblast-rich layer in both groups ($p < 0.05$) (Figure 7). The total cell count of Ki67-positive cells was higher in group A at every time point.

For the grade of inflammation shown by detection of CD68-positive cells as a representative staining for monocytes/macrophages, an opposing trend was seen in the collagenous layer. A lower cell count in group A after 3 weeks than that in group B was followed by an increase in inflammatory cells in group A and a decrease in group B after 12 weeks. Finally, the cell count in group A fell below the initial level after 52 weeks, and a strong increase in cells was observed in group B ($p < 0.05$) (Figure 8). A similar development was seen in the periprosthetic myofibroblast-rich layer, with the difference that there was no significant change in cell count in group B between 12 and 52 weeks (Figure 8).

As a sign of integration, the formation of blood vessels in the APD was analyzed. Overall, there was a statistically significant increase in blood vessels in the APD around the implants at all time points, developing from the adjacent tissue in the direction of the APD ($p < 0.05$) (Figure 9).

The analysis of the gene expression of the aforementioned target genes showed a distinctly lower mRNA expression for TGF β 1 in group A than in group B. With time, the expression showed a statistically significant drop ($p < 0.05$)

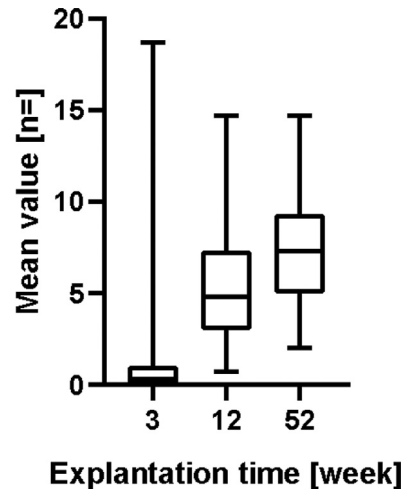


Figure 9 Results of blood vessel ingrowth in the APD after 3, 12, and 52 weeks.

(Figure 10). Similar data were collected for TNF α , where the expression rate in group A was always below that in group B (Figure 10). The expression rate of MMP1 was statistically significantly lower in group A at every time point

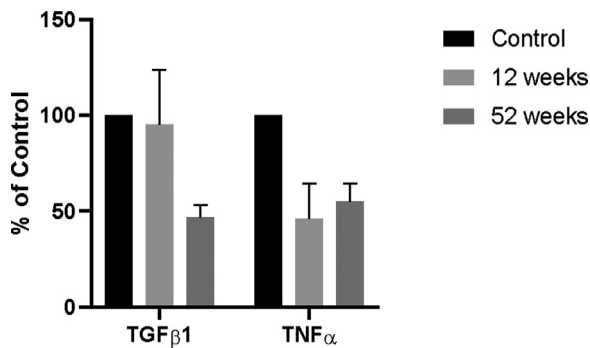


Figure 10 Results of gene expression of TGF β 1 after 12 and 52 weeks compared to the control group (left). Results of gene expression of TNF α after 12 and 52 weeks compared to the control group (right).

($p < 0.05$). Tissue inhibitors of metalloproteinase 1 (TIMP1) revealed inhomogeneous data, without an obvious difference between the groups. The calculated relation between MMP1 and TIMP1 showed a higher ratio in group A with time.

Discussion

Biologicals such as acellular dermal matrices are commonly used in breast augmentation and alloplastic breast reconstruction.^{16,17} A long-lasting support of the inframammary fold as well as the coverage of the lower pole of a silicone implant, along with dermal augmentation under the usually thin skin envelope, are the basic mechanisms of acellular dermal matrices, especially in reconstructive surgery after mastectomy. It has been hypothesized that a silicone implant covered by APD could prevent capsular contracture and would reduce the foreign body reaction, as well as the inflammatory response, acting as a biological barrier between the implant and the surrounding tissue.^{3,8}

Because the incidence of breast augmentations is still high and alloplastic breast reconstruction remains a common alternative compared to autologous breast reconstruction after mastectomy, plastic surgeons are confronted with the unsolved problem of capsular contracture. Tissue engineering might be an alternative in the future to overcome the problem of using allogeneic, xenogeneic, or artificial materials in this context.^{18,19} Clinical and observational studies emphasize the use of APD for the aforementioned indications, but long-term studies with molecular biological and immunohistochemical analysis are rare. Among the various allogeneic or xenogeneic materials that are commercially available, we chose a newly developed porcine matrix that is delivered as a sterile non-cross-linked acellular dermal matrix.

In this long-term experimental study, we analyzed multiple parameters commonly known to play a key role in the development of capsular contractures. Different cells are found to be predominant within breast capsular tissue. Particularly, the number of fibroblasts and the thickness of the collagenous layer have been reported to correlate with the Baker contraction grades.^{3,20,21} Furthermore, myofibroblasts have been considered as playing an important

role as progenitor cells and in stabilizing the capsular contracture.²² TGF β 1 and TNF α are well described as the main molecules involved in the modulation and formation of this disease.^{23,24} TGF β 1 acts as a potent fibrotic, angiogenic, and inflammatory mediator and plays a prominent role in fibrotic diseases, whereas TNF α is suggested as inhibiting the collagen synthesis at a transcriptional level, showing a pro-inflammatory activity.²⁴⁻²⁷ In this context, a decreased expression of these genes is assumed to correlate with an antifibrotic tendency.

To the best of our knowledge, this is the first experimental study with a follow-up of 52 weeks in an *in vivo* animal model in this context. With time, there are several changes at the molecular and histological levels, which are of interest in this context. Our study provides further and specific information that has not been described in other studies to date, probably because of the comparatively long duration of the experimental setting.^{25,28-31}

For the potential profibrotic parameters, notably, TGF β 1 and the thickness of the collagenous and the periprosthetic myofibroblast-rich layer, we found a statistically lower expression rate and development, respectively, in the experimental group (with APD). Similar results were seen for the assessed pro-inflammatory parameters. TNF α level and the number of CD68-positive cells in the collagenous and periprosthetic myofibroblast-rich layers were also statistically significant lower. Interestingly, significant and hitherto unknown differences between the groups at the histological and molecular biological levels only could be observed due to the long-term follow-up of this study. The thickness of the collagenous layer, for example, showed an increase after 12 weeks in both groups but dropped remarkably after 52 weeks, finally decreasing to a level lower than that at 3 weeks in the experimental group. CD 68-positive cells in the collagenous layer revealed an antipodal course with time in both groups. Although an increase in cell count was detected after 12 weeks in the experimental group compared to the 3-week count, CD68-positive cells in the control group initially dropped, showing a level lower than that in the experimental group. Contrary to this development, after 52 weeks, the cell count decreased to a level lower than that after 3 weeks in the experimental group and clearly increased in the control group to reach more than twice the cell count of the experimental group. Similar results were observed for the CD68-positive cells in the periprosthetic myofibroblast-rich layer after 3 and 12 weeks. Here, the cell count also showed a distinct decrease in the experimental group after 52 weeks, whereas the cell count presented as unchanged in the control group. These descriptive results underline the hypothesis of a latent chronic inflammatory influence in the etiology of capsular contracture.

The continuous ingrowth of blood vessels observed in the experimental group, together with an expansion toward the implant, may be interpreted as a clear sign for integration of the matrix. Furthermore, this could explain the higher rate of proliferating cells than that of the control group.

In addition, the role of the remodeling of ECM is known as an indicator of fibrotic activity in the development of capsular contracture in general. Matrix metalloproteinases (MMPs) are major enzymes in ECM degradation and are regulated by two major endogenous inhibitors: α ₂-macroglobulin and tissue inhibitors of metalloproteinases

(TIMPs).³²⁻³⁴ ECM degradation and collagenous remodeling could be considered as an important process in capsular fibrosis. Therefore, a high expression of MMPs and low expression of TIMPs would be comprehensible for active ECM remodeling. Furthermore, a pathological accumulation of collagen is attributed to the dysregulation of MMP expression.³⁵ Moreover, MMPs are known to exacerbate inflammation and fibrosis due to excessive and unregulated destruction and remodeling of ECM.^{36,37} MMP1 as interstitial collagenase is involved in tissue maintenance and wound repair.³⁸⁻⁴⁰ An elevated systemic TIMP1 concentration can be observed in severe fibroproliferative disorders.^{41,42} Little is known about the activation and influence of MMP1 in capsular tissue. Serum concentrations of female patients showed no significant difference in MMP1 levels compared to those of patients after reduction mammoplasty, whereas MMP2 revealed a significant increase.⁴³ Kyle et al. found an upregulation of MMP12 in contracted breast capsule tissue from patients after preselection of target genes using a genome microarray analysis.³⁶ In their study, TIMP4 showed no significant regulation, similar to our results.

The MMP1 protein functions as an interstitial collagenase to break down interstitial collagen types I, II, and III.^{44,45} Focusing on the analysis of APD and adjacent tissue next to the silicone implant, the expression of MMP1 may play a relevant role. Because MMP1 showed a level lower than that of the control group and TIMP1 revealed no remarkable difference, this could be a key finding. Although not statistically significant, the concentration of MMP1 in the experimental group may thus indicate a reduced activity due to a lower collagen deposition adjacent to the APD. Consequently, one can hypothesize that APD might lead to a lower collagen deposition and lower extracellular activity as well as inflammation, resulting in reduced or stable MMP1 expression. Assuming this, the initial trigger for an increased MMP1 activation might be disregarded.

This can also be speculated for the MMP1-to-TIMP1 ratio, which we found to show a higher expression level in the experimental group. As seen in previous studies focusing on fibrotic diseases, decreased levels were accompanied with severe fibrotic activity and increased synthesis and deposition of collagen.^{32,41,43,46,47} Furthermore, Ulrich et al. described a lower MMP1-to-TIMP1 ratio in patients with capsular contracture after breast augmentation, which correlated with the Baker classification.³² In the context of this study, the higher ratio may, therefore, be interpreted as antifibrotic tendency induced by APD.

Conclusion

In this long-term *in vivo* study, we found an antifibrotic effect by completely wrapping silicone gel implants with APD on immunohistochemical and molecular biological levels. Relevant changes in fibrotic and inflammatory markers in the surrounding tissue could be demonstrated in the long-term 1-year follow-up. Assuming a latent inflammatory etiology of capsular contracture, this study provides important results for assessing the potential benefits of APD. We conclude that further clinical and experimental studies should focus on long-term follow-ups for more detailed results.

Transferred to the clinical application of this concept, one may hypothesize that using APD together with silicone implants could have a positive impact on the development of capsular contracture. Further clinical studies are required to corroborate these experimental data in the future.

Conflict of interest statement

The authors received financial funding for this investigator-driven study by Tutogen Medical GmbH (subsidiary of RTI Surgical®, Alachua, FL, USA).

R.E. Horch has performed investor-initiated studies and served as lecturer and advisor to KCI, Baxter, and Tutogen Medical GmbH.

M. Schmitz performed investor-initiated studies for LifeCell™.

Furthermore, there are no conflicts of interest for one of the authors.

Acknowledgments

Parts of the present work were performed in fulfillment of the requirements for obtaining the doctoral title “Dr. med.”

References

1. Maxwell GP, Gabriel A. Acellular dermal matrix for reoperative breast augmentation. *Plast Reconstr Surg* 2014;134:932-8.
2. Dickinson BP, Handel N. Approaching revisional surgery in augmentation and mastopexy/augmentation patients. *Ann Plast Surg* 2012;68:12-16.
3. Headon H, Kasem A, Mokbel K. Capsular contracture after breast augmentation: an update for clinical practice. *Arch Plast Surg* 2015;42:532-43.
4. Becker H, Lind JG 2nd. The use of synthetic mesh in reconstructive, revision, and cosmetic breast surgery. *Aesthet Plast Surg* 2013;37:914-21.
5. Vu MM, Kim JY. Current opinions on indications and algorithms for acellular dermal matrix use in primary prosthetic breast reconstruction. *Gland Surg* 2015;4:195-203.
6. Steiert AE, Boyce M, Sorg H. Capsular contracture by silicone breast implants: possible causes, biocompatibility, and prophylactic strategies. *Med Devices (Auckl)* 2013;6:211-18.
7. Anderson JM, Rodriguez A, Chang DT. Foreign body reaction to biomaterials. *Semin Immunol* 2008;20:86-100.
8. Schmitz M, Bertram M, Kneser U, Keller AK, Horch RE. Experimental total wrapping of breast implants with acellular dermal matrix: a preventive tool against capsular contracture in breast surgery? *J Plast Reconstr Aesthet Surg* 2013;66:1382-9.
9. Seyhan H, Kopp J, Beier JP, et al. Smooth and textured silicone surfaces of modified gel mammary prostheses cause a different impact on fibroproliferative properties of dermal fibroblasts. *J Plast Reconstr Aesthet Surg* 2011;64:e60-6.
10. Yang JD, Kwon OH, Lee JW, et al. The effect of montelukast and antiadhesion barrier solution on the capsule formation after insertion of silicone implants in a white rat model. *Eur Surg Res* 2013;51:146-55.
11. Moreira M, Fagundes DJ, de Jesus Simoes M, et al. The effect of liposome-delivered prednisolone on collagen density, myofibroblasts, and fibrous capsule thickness around silicone breast implants in rats. *Wound Repair Regen* 2010;18:417-25.

12. Selber JC, Wren JH, Garvey PB, et al. Critical evaluation of risk factors and early complications in 564 consecutive two-stage implant-based breast reconstructions using acellular dermal matrix at a single center. *Plast Reconstr Surg* 2015;136:10-20.
13. Glasberg SB, Light D. AlloDerm and strattice in breast reconstruction: a comparison and techniques for optimizing outcomes. *Plast Reconstr Surg* 2012;129:1223-33.
14. Ng CE, Pieri A, Fasih T. Porcine acellular dermis-based breast reconstruction: complications and outcomes following adjuvant radiotherapy. *Eur J Plast Surg* 2015;38:459-62.
15. Hille-Betz U, Kniebusch N, Wojcinski S, et al. Breast reconstruction and revision surgery for implant-associated breast deformities using porcine acellular dermal matrix: a multicenter study of 156 cases. *Ann Surg Oncol* 2015;22:1146-52.
16. Kim JYS, Mlodinow AS. What's new in acellular dermal matrix and soft-tissue support for prosthetic breast reconstruction. *Plast Reconstr Surg* 2017;140:305-43S.
17. Sorokin M, Qi J, Kim HM, et al. Acellular dermal matrix in immediate expander/implant breast reconstruction: a multicenter assessment of risks and benefits. *Plast Reconstr Surg* 2017;140:1091-100.
18. Arkudas A, Lipp A, Buehrer G, et al. Pedicled transplantation of axially vascularized bone constructs in a critical size femoral defect. *Tissue Eng Part A* 2017.
19. Yuan Q, Arkudas A, Horch RE, et al. Vascularization of the arteriovenous loop in a rat isolation chamber model-quantification of hypoxia and evaluation of its effects. *Tissue Eng Part A* 2017.
20. Brazin J, Malliaris S, Groh B, et al. Mast cells in the periprosthetic breast capsule. *Aesthet Plast Surg* 2014;38:592-601.
21. Spear SL, Baker JL Jr. Classification of capsular contracture after prosthetic breast reconstruction. *Plast Reconstr Surg* 1995;96:1119-23 discussion 24.
22. Persichetti P, Segreto F, Carotti S, et al. Oestrogen receptor-alpha and -beta expression in breast implant capsules: experimental findings and clinical correlates. *J Plast Reconstr Aesthet Surg* 2014;67:308-15.
23. Katzel EB, Koltz PF, Tierney R, et al. The impact of Smad3 loss of function on TGF-beta signaling and radiation-induced capsular contracture. *Plast Reconstr Surg* 2011;127:2263-9.
24. Tan KT, Wijeratne D, Shih B, Baildam AD, Bayat A. Tumour necrosis factor-alpha expression is associated with increased severity of periprosthetic breast capsular contracture. *Eur Surg Res* 2010;45:327-32.
25. Diao ZY, Fu HL, Nie CL, et al. Controlled release of transforming growth factor-beta receptor kinase inhibitor from thermosensitive Chitosan-based hydrogel: application for prevention of capsular contracture. *Chin Med J (Engl)* 2011;124:284-90.
26. D'Andrea F, Nicoletti GF, Grella E, et al. Modification of cysteinyl leukotriene receptor expression in capsular contracture: preliminary results. *Ann Plast Surg* 2007;58:212-14.
27. Chakraborty D, Sumova B, Mallano T, et al. Activation of STAT3 integrates common profibrotic pathways to promote fibroblast activation and tissue fibrosis. *Nat Commun* 2017;8:1130.
28. Marques M, Brown S, Correia-Sa I, et al. The impact of triamcinolone acetonide in early breast capsule formation in a rabbit model. *Aesthetic Plast Surg* 2012;36:986-94.
29. Vieira VJ, d'Acampora AJ, Marcos AB, et al. Vascular endothelial growth factor overexpression positively modulates the characteristics of periprosthetic tissue of polyurethane-coated silicone breast implant in rats. *Plast Reconstr Surg* 2010;126:1899-910.
30. Reichenberger MA, Heimer S, Lass U, et al. Pulsed acoustic cellular expression (PACE) reduces capsule formation around silicone implants. *Aesthetic Plast Surg* 2014;38:244-51.
31. Ruiz-de-Erenchun R, Dotor de las Herrerias J, Hontanilla B. Use of the transforming growth factor-beta1 inhibitor peptide in periprosthetic capsular fibrosis: experimental model with tetraglycerol dipalmitate. *Plast Reconstr Surg* 2005;116:1370-8.
32. Ulrich D, Ulrich F, Pallua N, Eisenmann-Klein M. Effect of tissue inhibitors of metalloproteinases and matrix metalloproteinases on capsular formation around smooth and textured silicone gel implants. *Aesthetic Plast Surg* 2009;33:555-62.
33. Lichtinghagen R, Michels D, Haberkorn CI, et al. Matrix metalloproteinase (MMP)-2, MMP-7, and tissue inhibitor of metalloproteinase-1 are closely related to the fibroproliferative process in the liver during chronic hepatitis C. *J Hepatol* 2001;34:239-47.
34. Weigand A, Boos AM, Tasbihi K, et al. Selective isolation and characterization of primary cells from normal breast and tumors reveal plasticity of adipose derived stem cells. *Breast Cancer Res* 2016;18:32.
35. Davis ME, Gumucio JP, Sugg KB, Bedi A, Mendias CL. MMP inhibition as a potential method to augment the healing of skeletal muscle and tendon extracellular matrix. *J Appl Physiol (1985)* 2013;115:884-91.
36. Kyle DJ, Harvey AG, Shih B, et al. Identification of molecular phenotypic descriptors of breast capsular contracture formation using informatics analysis of the whole genome transcriptome. *Wound Repair Regen* 2013;21:762-9.
37. Belvisi MG, Bottomley KM. The role of matrix metalloproteinases (MMPs) in the pathophysiology of chronic obstructive pulmonary disease (COPD): a therapeutic role for inhibitors of MMPs? *Inflamm Res* 2003;52:95-100.
38. Lee SG, Lee SD, Kim MK, et al. Effect of antiadhesion barrier solution and fibrin on capsular formation after silicone implant insertion in a white rat model. *Aesthetic Plast Surg* 2015;39:162-70.
39. Armstrong DG, Jude EB. The role of matrix metalloproteinases in wound healing. *J Am Podiatr Med Assoc* 2002;92:12-18.
40. Ravanti L, Kahari VM. Matrix metalloproteinases in wound repair (review). *Int J Mol Med* 2000;6:391-407.
41. Ulrich D, Hrynyschyn K, Pallua N. Matrix metalloproteinases and tissue inhibitors of metalloproteinases in sera and tissue of patients with Dupuytren's disease. *Plast Reconstr Surg* 2003;112:1279-86.
42. Anik I, Kokturk S, Genc H, et al. Immunohistochemical analysis of TIMP-2 and collagen types I and IV in experimental spinal cord ischemia-reperfusion injury in rats. *J Spinal Cord Med* 2011;34:257-64.
43. Ulrich D, Lichtenegger F, Eblenkamp M, Repper D, Pallua N. Matrix metalloproteinases, tissue inhibitors of metalloproteinases, aminoterminal propeptide of procollagen type III, and hyaluronan in sera and tissue of patients with capsular contracture after augmentation with Trilucent breast implants. *Plast Reconstr Surg* 2004;114:229-36.
44. Forrester HB, Temple-Smith P, Ham S, et al. Genome-wide analysis using exon arrays demonstrates an important role for expression of extra-cellular matrix, fibrotic control and tissue remodelling genes in Dupuytren's disease. *PLoS One* 2013;8:e59056.
45. Huang SF, Li YH, Ren YJ, Cao ZG, Long X. The effect of a single nucleotide polymorphism in the matrix metalloproteinase-1 (MMP-1) promoter on force-induced MMP-1 expression in human periodontal ligament cells. *Eur J Oral Sci* 2008;116:319-23.
46. Ulrich D, Ulrich F, Piatkowski A, Pallua N. Expression of matrix metalloproteinases and their inhibitors in cords and nodules of patients with Dupuytren's disease. *Arch Orthop Trauma Surg* 2009;129:1453-9.
47. Polyakova V, Hein S, Kostin S, Ziegelhoeffer T, Schaper J. Matrix metalloproteinases and their tissue inhibitors in pressure-overloaded human myocardium during heart failure progression. *J Am Coll Cardiol* 2004;44:1609-18.